

High Resolution 3D TrueFISP images of Guinea Pig Inner Ear using the Composite Gradient Systems on a Clinical 3T MRI System

Seong-Eun Kim¹, K Craig Goodrich¹, Richard Wiggins¹, Jason Mendes¹, and Dennis L Parker¹
¹UCAIR Department of Radiology, University of Utah, Salt Lake City, Utah, United States

Introduction: Imaging of the inner ear requires a high degree of anatomic detail to understand and diagnose certain pathologies¹⁻³. At the resolution desired for many inner ear pathologies, limits on gradient performance require pulse sequence compromises including an increased TR in SSFP sequences, causing banding artifacts that can mask diagnostic information⁴. If magnetic field inhomogeneity causes a larger frequency variation in the imaging volume than $1/TR$, dark banding is observed. Improved gradient performance can allow shorter TR's for SSFP sequences where the frequency bandwidth that can be imaged without artifact is $1/TR$. Thus, improved gradient performance will result in increased signal to noise ratio (SNR) and reduced banding artifacts in SSFP images, both of which are critical for imaging the fine detail in the inner and middle ear⁵. To test this hypothesis a local head and neck insert gradient has been developed for simultaneous use with the whole body gradients in a 3T research MRI scanner. Our composite gradient system that combines the system body gradients simultaneously with the insert gradient can achieve improved performance by nearly a factor of 3 in speed and amplitude over the body gradients alone. The use of composite gradients will allow high resolution SSFP images without increasing TR or bandwidth, allowing for improved inner ear imaging. To test the utility of this composite gradient system we scanned the temporal bone of guinea pigs with the composite and body gradients only and compared image quality.

Methods: The head neck insert coil was constructed based on a design obtained using the Boundary Element (BE) method⁶. All MRI scans were performed on a Siemens 3Tesla TIM Trio scanner, where the standard system was augmented with three additional gradient amplifiers and master/slave configured computers capable of controlling extra gradient channels. The control hardware and software were developed and provided by Siemens. Pulse sequences were implemented to control both gradient coils synchronously. The master computer was used to 1) maintain all computer controlled shims, including the first order gradient shims obtained using the standard body gradients, 2) control RF excitation and reception, 3) control standard whole body imaging gradients, and 4) synchronously trigger the slave computer. The slave computer executed a pulse sequence controlling the insert gradients. T2w images of the deceased guinea pig was acquired using the 3D TrueFISP sequence and composite gradients (with insert and body at the same strength) with the following parameters: matrix=256x152, FA=50° and bandwidth = 266 Hz/pixel. The isotropic voxel size was 0.4 mm³. The same acquisition was performed on the body gradients with adjustments of imaging parameters such as FOV, slice thickness and TE/TR to obtain the same 0.4 mm³ voxel resolution used in the composite gradients. Multiple phase cycled images were acquired using four different phase increments, 0°, 90°, 180°, and 270°, to reduce the banding artifact and noise more reliably⁷.

Results: Table 1 summarized TE/TR used in composite and body gradients.

Table 1 3D TrueFISP Imaging Parameters		
	TE/TR (ms)	Scan Time(min)
Composite Gradients	3.0/6.0	4:32
Body Gradients	4.12/8.25	6:04

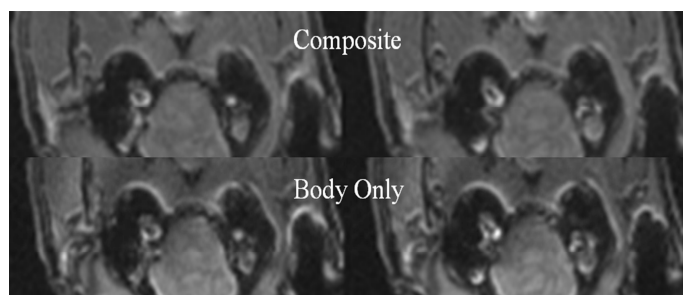


Figure 1: Trufi images of normal guinea pig cochlea with multiple phase cycling using composite (top) body (bottom) gradients system

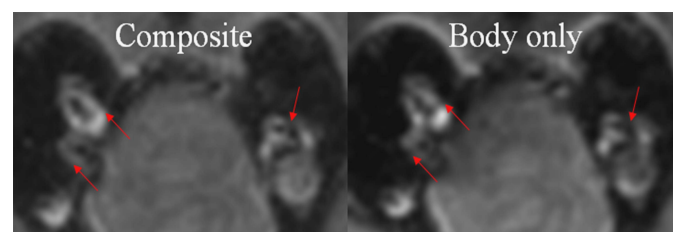


Figure 2: Enlargement of inner ear images obtained from composite (right) and body gradients. The image obtained from body gradients still suffers from banding artifacts (see red arrows).

Fig 1 displays TrueFISP images of guinea pig using composite (top) and body (bottom) gradients. Fig 2 shows the enlargement of image seen in Fig 1 obtained from composite (right) and body (left) gradients. The image obtained from body gradients still suffers from band artifacts (see red arrows).

Discussion: Results from this early work in guinea pigs are promising in that the improved imaging quality in high resolution TrueFISP images seen with the composite gradient system not only demonstrates better visualization of the inner ear structure with less banding artifacts, but may actually allow for scan time reduction. High resolution imaging of the inner ear in humans is but one potential utility of this novel system which allows for the simultaneous use of composite gradients. This system would be particularly useful clinically in that in addition to the improved imaging obtained with the composite system over insert gradient coils alone, it would allow for the use of body gradients alone for conventional clinical studies without the need for removing the insert gradients. Our hope is to develop imaging protocols for human temporal bone studies using a high field (3T) human whole body scanner with a head neck insert gradient coil operating simultaneously in a dual gradient mode. These early comparisons showing improved visualization of inner ear infrastructure in animals are evidence of the potential of this system to resolve the fine detail of the human inner ear in a way in which there may at last be an objective test for the diagnosis of inner ear pathology. Note that in these studies, the insert gradient was operated at half of its full potential gradient strength, and therefore, further shortening of the repetition time in TrueFISP imaging can be expected.

References

1. Counter SA, et al. *Neuroreport*, **11**(18): p. 3979-83(2000).
2. Niyazov DM, et al. *Otol Neurotol*. **22**(6): p. 813-7(2001).
3. Silver RD, et al. *Laryngoscope*. **112**(10): p. 1737-41(2002).
4. Hans P, et al. *AJNR Am J Neuroradiol*. **20**(7):1197-1206(1999).
5. Parker DL, et al. *Concepts Magn Reson Part B Magn Reson Eng*. **35**(2):89-97(2009).
6. Handler WB, Dalymple B, Goodrich CK, et al. *Proc. Intl. Soc. Mag. Reson. Med*. **19**:1834(2011).
7. Jung K-J, *Magnetic Resonance Imaging*. **28**:103-118(2010).

Acknowledgements: This work is supported by the Ben B. and Iris M. Margolis Foundation and Siemens Health Care AG, and NIH R33 EB009082.